J Therm Anal Calorim (2014) 116:779–783
DOI 10.1007/s10973-013-3566-5

Thermodynamic properties and phase transitions of Tutton salt $(NH_4)_2Fe(SO_4)_2{\cdot}6H_2O$ from MAS NMR and single-crystal NMR

Woo Young Kim · Ae Ran Lim

Received: 6 October 2013 / Accepted: 26 November 2013 / Published online: 11 December 2013

Abstract The thermodynamic properties and phase transitions of Tutton salt $(NH_4)_2Fe(SO_4)_2{\cdot}6H_2O$ were investigated using thermogravimetric analysis, differential scanning calorimetry, and nuclear magnetic resonance. The first mass loss occurs around 330 K (T_d), which is interpreted as the onset of partial thermal decomposition. Phase transitions were found at 387 K ($=T_{C1}$) and 500 K ($=T_{C2}$). The temperature dependences of the spin–lattice relaxation time in the rotating frame, $T_{1\rho}$, and that in the laboratory frame, T_1, for the H nuclei change abruptly near T_{C1}. These changes are associated with changes in the geometry of the arrangement of octahedral water molecules and ammonium protons.

Keywords Tutton salts · $(NH_4)_2Fe(SO_4)_2{\cdot}6H_2O$ · Thermodynamic property · MAS NMR · Solid NMR · Phase transition

Introduction

Tutton salts have played a significant role in physics and chemistry; considerable attention is currently focused on the development of materials suitable for strong energy absorption by solar collectors. For domestic heating and hot water supplies, this energy might be stored chemically in reversible reactions or thermally in phase changes or temperature increases of the storage materials [1, 2]. Tutton salts are an isomorphous series of monoclinic crystals with the general formula $M^I_2M^{II}(SO_4)_2{\cdot}6H_2O$. They contain two octahedral hexahydrate complexes $[M^{II}(H_2O)_6]^{2+}$ in the crystal unit cell, where M^{II} is a divalent cation (Co, Zn, Fe, or an ion of the 3*d* group), and M^I is a monovalent cation (K, Rb, Cs, or NH_4) [3–10]. The unit cell dimensions and molecular structures of the crystals of this family are very similar. Montgomery and Lingafelter described the structural characteristics of the crystals in this series, including the details of their hydrogen bond networks [11]. One $M^I_2M^{II}(SO_4)_2{\cdot}6H_2O$ compound, $(NH_4)_2Fe(SO_4)_2{\cdot}6H_2O$, has a monoclinic structure with space group $P2_1/a$. Six water molecules surround the divalent inversion symmetric sites. The divalent atoms in the unit cell are located at (0, 0, 0) and (½, ½, 0), whereas all the other atoms are in general positions.

Previous study has reported the physical properties; the thermal decomposition of $(NH_4)_2Fe(SO_4)_2{\cdot}6H_2O$ has been studied and identified using the Mössbauer effect, X-ray diffraction, infrared spectroscopy, gravimetric, and thermal differential methods [12]. Recently, Ganesh et al. [13] investigated thermal behavior and dielectric characterization of $(NH_4)_2Fe(SO_4)_2{\cdot}6H_2O$ single crystal.

The interesting properties of Tutton salts have been studied by many methods in recent years. However, the thermodynamic properties and phase transition temperatures of $(NH_4)_2Fe(SO_4)_2{\cdot}6H_2O$ crystals have not been reported. Further, some questions about Tutton salts remain open, especially those related to the nature of their structural changes and their thermodynamic properties. The hydrogen bond protons in $(NH_4)_2Fe(SO_4)_2{\cdot}6H_2O$ crystals are expected to play a dominant role in their physical properties and phase transition mechanisms. The relationship between the loss of water protons and structural phase

W. Y. Kim · A. R. Lim
Department of Carbon Fusion Engineering, Jeonju University, Jeonju 560-759, Korea

A. R. Lim (✉)
Department of Science Education, Jeonju University, Jeonju 560-759, Korea
e-mail: aeranlim@hanmail.net; arlim@jj.ac.kr

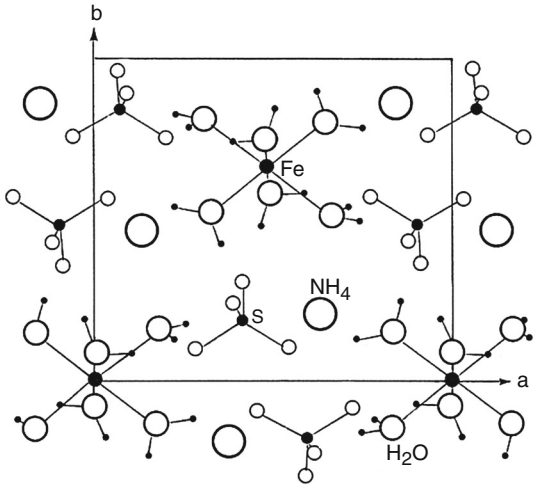

Fig. 1 Crystal structure of $(NH_4)_2Fe(SO_4)_2{\cdot}6H_2O$ projected onto the *ab* plane

transitions is a subject of keen interest. To probe the variations with temperature in the physical properties of $(NH_4)_2Fe(SO_4)_2{\cdot}6H_2O$ crystals, studying the ^1H NMR spectrum and relaxation times is preferable because they are likely to be very sensitive to changes in the symmetry of the crystal.

This paper discusses the thermodynamic properties on the basis of differential scanning calorimetry (DSC) and thermogravimetric analysis (TG) measurements. In addition, the temperature dependences of the spin–lattice relaxation time in the rotating frame, $T_{1\rho}$, and that in the laboratory frame, T_1, for the ^1H nuclei in $(NH_4)_2Fe(SO_4)_2{\cdot}6H_2O$ were investigated using a pulse nuclear magnetic resonance (NMR) spectrometer to obtain detailed information about the physical properties. This is the first investigation of the structural changes in $(NH_4)_2Fe(SO_4)_2{\cdot}6H_2O$ crystals, and we use these results to analyze the environments of their ^1H nuclei. It is noteworthy that their thermodynamic properties and phase transitions were studied by analyzing these environments.

Crystal structure

$(NH_4)_2Fe(SO_4)_2{\cdot}6H_2O$ single crystals have monoclinic structure with space group $P2_1/a$ and lattice parameters $a = 6.2383$ Å, $b = 12.6076$ Å, $c = 9.2652$ Å, $\alpha = \gamma = 90°$, and $\beta = 106.524°$ [14]. The unit cell contains two Fe^{2+} ions, each surrounded by six water molecules forming an octahedron, as shown in Fig. 1. $(NH_4)_2Fe(SO_4)_2{\cdot}6H_2O$ is built up from $Fe(H_2O)_6$ octahedra, SO_4 square planar forms, and NH_4 tetrahedra. The $Fe(H_2O)_6$ octahedra is highly distorted, as indicated by the Fe–O bond. Each $[Fe(H_2O)_6]^{2+}$ complex cation is surrounded by four sulfate anion acceptor groups and four ammonium cation donor groups. The crystal structure is stabilized by the N–H···O and O–H···O hydrogen bonds viewed along the *a*-axis.

Experimental

Single crystals of $(NH_4)_2Fe(SO_4)_2{\cdot}6H_2O$ were grown by slow evaporation from an aqueous solution at 293 K. The resulting single crystals were hexagonal shape and jade green color with a size of $\sim 4 \times 7 \times 3$ mm^3.

The ^1H magic angle spinning (MAS) NMR spectrum and the spin–lattice relaxation time $T_{1\rho}$ in the rotating frame were measured in $(NH_4)_2Fe(SO_4)_2{\cdot}6H_2O$ by the Varian 200 MHz NMR spectrometer at the Korea Basic Science Institute. The Larmor frequency was set to 200 MHz, and the sample powder was placed in a 4 mm MAS probe. The rotor was spun at 10 kHz to minimize spinning sideband overlap. $T_{1\rho}$ was measured by varying the duration of a ^1H spin-locking pulse applied after direct polarization, i.e., through $\pi/2$–τ acquisition. The $\pi/2$ pulse time for ^1H was 2.7 μs, which was equivalent to a spin-locking field strength of 92.59 kHz. In addition, the ^1H NMR spectrum and spin–lattice relaxation time T_1 in the laboratory frame were obtained in $(NH_4)_2Fe(SO_4)_2{\cdot}6H_2O$ single crystals. The spin–lattice relaxation time was measured using a saturation recovery pulse sequence, π–τ–$\pi/2$ acquisition; the nuclear magnetizations of the ^1H nuclei at time τ after the *sat* pulse were determined following the $\pi/2$ excitation pulse. The width of the π pulse was 2.5 μs for ^1H. Temperature-dependent NMR measurements were conducted at 200–400 K. The sample temperature was maintained at the required constant value with an accuracy of ±0.5 °C by controlling the helium gas flow and heater current.

Experimental results and discussion

To determine the structure of a single $(NH_4)_2Fe(SO_4)_2{\cdot}6H_2O$ crystal, X-ray diffractometry was performed using the Bruker AXS GMBH instrument with a Cu target at the Korea Basic Science Institute. The crystal structure is monoclinic, and the lattice constants are $a = 6.245$ Å, $b = 12.591$ Å, $c = 9.287$ Å, $\alpha = \gamma = 90°$, and $\beta = 106.784°$. Further, the space group is obtained as $P2_1/c$. These results are consistent with the data of Ganesh et al. [13]. In addition, DSC (DuPont 2010 DSC) was used to determine the phase transition temperatures of the crystals. The measurement was performed at a heating rate of 10 °C min^{-1}. Endothermic and exothermic peaks were observed at 387 and 500 K, respectively, as shown in Fig. 2. This result is consistent with the 381.7 K reported by Voight and Goring [15]. TG was then used to determine whether these high-temperature transformations are structural phase

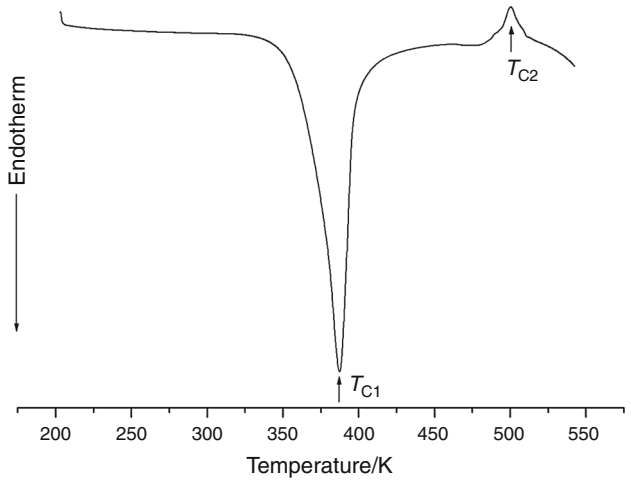

Fig. 2 Differential scanning calorimetry curve of $(NH_4)_2Fe(SO_4)_2{\cdot}6H_2O$ single crystal

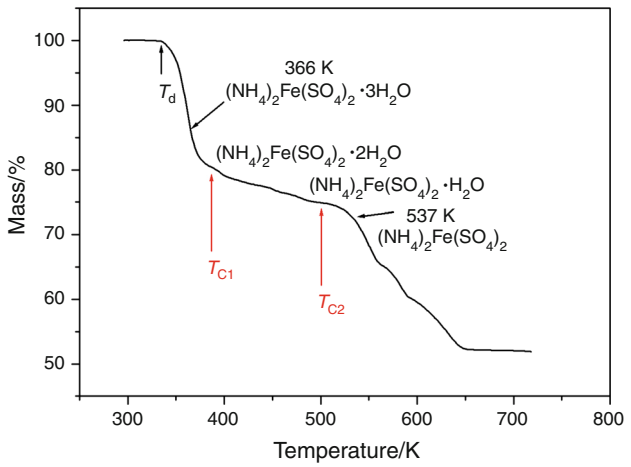

Fig. 3 Thermogravimetric analysis of $(NH_4)_2Fe(SO_4)_2{\cdot}6H_2O$ crystal

transitions or chemical reactions. The curve of $(NH_4)_2Fe(SO_4)_2{\cdot}6H_2O$ is shown in Fig. 3. The first mass loss begins around 330 K and reaches 14 % as $(NH_4)_2Fe(SO_4)_2{\cdot}3H_2O$ at 366 K. Near 537 K, the thermal decomposition enters a new stage, and the residue of the final products reaches a value of 72.15 %, accompanied by the escape of H_2O. Optical polarizing microscopy shows that the crystals are jade green color at room temperature and that their color changes to white with increasing temperature. This color change may be related to the loss of H_2O. The bulk mass of $(NH_4)_2Fe(SO_4)_2{\cdot}6H_2O$ decreases at 330 K (T_d), which is interpreted as the onset of partial thermal decomposition, and reaches complete thermal decomposition into $(NH_4)_2Fe(SO_4)_2$ around 537 K. The DSC, TG, and optical polarizing microscopy results for $(NH_4)_2Fe(SO_4)_2{\cdot}6H_2O$ crystals show that the mass loss around 330 K (=T_d) is due to the onset of partial thermal decomposition. The transformation anomalies at 387 K (= T_{C1}) and 500 K (= T_{C2}) are related to

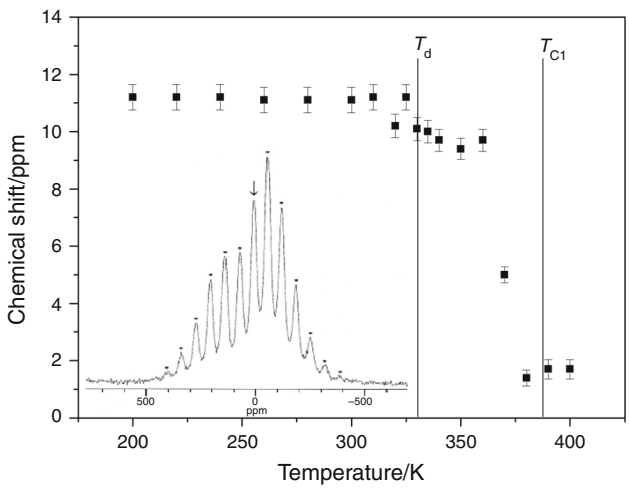

Fig. 4 Chemical shift of ^1H signal as a function of temperature (*inset* ^1H MAS NMR spectrum of $(NH_4)_2Fe(SO_4)_2{\cdot}6H_2O$ at room temperature)

phase transitions from $(NH_4)_2Fe(SO_4)_2{\cdot}6H_2O$ to $(NH_4)_2Fe(SO_4)_2{\cdot}2H_2O$, and from $(NH_4)_2Fe(SO_4)_2{\cdot}6H_2O$ to $(NH_4)_2Fe(SO_4)_2{\cdot}H_2O$, respectively.

Structural analysis of the protons in $(NH_4)_2Fe(SO_4)_2{\cdot}6H_2O$ was conducted using solid-state NMR. The ^1H MAS NMR spectrum of $(NH_4)_2Fe(SO_4)_2{\cdot}6H_2O$ at room temperature is shown in the inset in Fig. 4. The NMR spectrum consists of one peak at a chemical shift of $\delta = 11.1$ ppm, and this signal is associated with the ammonium and hydrogen bond protons. The spinning sidebands are marked with asterisks. Here, the signals for the two types of protons cannot be distinguished because they overlap. The temperature dependence of the chemical shift in the ^1H NMR signal with respect to a reference signal is presented in Fig. 4. The chemical shift is generally sensitive to the electrical environment of the nucleus. Near T_{C1}, the chemical shift abruptly changes with increasing temperature, which is due to the phase transition. The shift in the resonance lines of $(NH_4)_2Fe(SO_4)_2{\cdot}6H_2O$ might be due to the dipole–dipole interactions between the magnetic moments of the H^+ nuclei and the magnetic moments of the Fe^{2+} atoms. The chemical shift near T_d is the beginning of a decrease of H_2O.

The spin–lattice relaxation time $T_{1\rho}$ in the rotating frame for the protons as a function of temperature was studied. The nuclear magnetization recovery traces obtained for protons at all temperatures are described by the following single exponential function: $M(t) = M_o\exp(-t/T_{1\rho})$, where $M(t)$ is the magnetization at time t, and M_o is the total nuclear magnetization of ^1H at thermal equilibrium [16]. The slopes of the recovery trace are different at several temperatures; one of them is shown in the inset in Fig. 5. The temperature dependence of $T_{1\rho}$ for the protons is shown in Fig. 5. The $T_{1\rho}$ value of the protons in $(NH_4)_2Fe(SO_4)_2{\cdot}6H_2O$ did not change significantly near T_d,

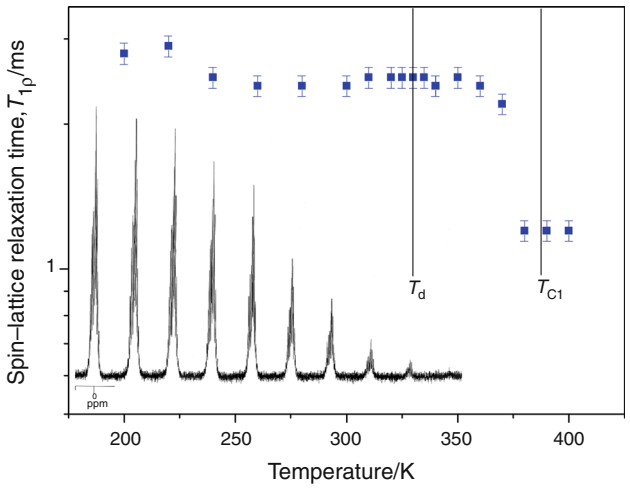

Fig. 5 Temperature dependence of spin–lattice relaxation time $T_{1\rho}$ in the rotating frame for the ^{1}H nuclei in $(NH_4)_2Fe(SO_4)_2{\cdot}6H_2O$ (*inset* recovery traces of ^{1}H as functions of delay time at room temperature)

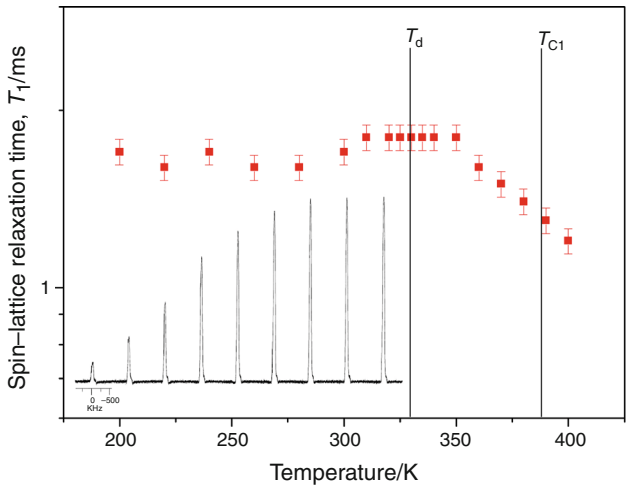

Fig. 7 Temperature dependence of spin–lattice relaxation time T_1 in the laboratory frame for ^{1}H nuclei in $(NH_4)_2Fe(SO_4)_2{\cdot}6H_2O$ single crystal (*inset* saturation recovery traces of ^{1}H as functions of the delay time at room temperature)

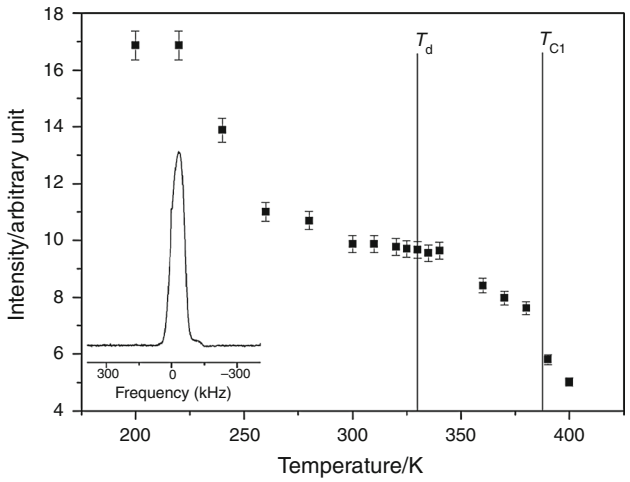

Fig. 6 Intensity of ^{1}H NMR spectra of $(NH_4)_2Fe(SO_4)_2{\cdot}6H_2O$ single crystal at room temperature (*inset* ^{1}H NMR spectra of $(NH_4)_2Fe(SO_4)_2{\cdot}6H_2O$ single crystal at room temperature)

but it decreased considerably near the phase transition temperature of T_{C1}, in addition to the change in the chemical shift at T_{C1}.

The NMR spectrum for the ^{1}H nuclei in a single $(NH_4)_2Fe(SO_4)_2{\cdot}6H_2O$ crystal was measured at various temperatures. As mentioned above, there are two types of protons in $(NH_4)_2Fe(SO_4)_2{\cdot}6H_2O$: ammonium protons, the relaxation of which is determined mainly by the hindered rotation of the NH_4 groups, and hydrogen bond protons, the relaxation of which is determined mainly by the motion of the hydrogens in H_2O. In our results, the proton signals due to the ammonium and hydrogen bond protons overlap, as shown in the inset in Fig. 6, and the line width due to the ammonium and hydrogen bond protons is very broad (70 kHz) at 300 K. Therefore, we cannot distinguish the two types. As the temperature is increased, the intensity of the signal decreases, as shown in Fig. 6, and it becomes quite weak above T_{C1}, which indicates that the protons play an important role in this phase transition. We conclude that the decrease in the intensity of the signal with temperature is related to the loss of H_2O.

The ^{1}H spin–lattice relaxation time T_1 in the laboratory frame was obtained for a single $(NH_4)_2Fe(SO_4)_2{\cdot}6H_2O$ crystal at a frequency of 200 MHz. Here, the magnetic field was applied along the *c*-axis of the crystal. The saturation recovery traces of the magnetization of ^{1}H at several different temperatures were measured. The measured magnetization recovery was found to be satisfactorily fitted with the single exponential function $[M(\infty) - M(t)]/M(\infty) = \exp(-Wt)$, where $M(t)$ is the nuclear magnetization at time t, and W is the transition probability corresponding to $\Delta m = \pm 1$. The relaxation time is given by $T_1 = 1/W$ [17]. The magnetization recovery at room temperature is shown in the inset in Fig. 7. The slopes of the recovery traces at each temperature are different. The variation in the proton dynamics of the hydrogen bond networks is associated with the phase transition. The ^{1}H relaxation time was obtained in terms of W, and the spin–lattice relaxation time T_1 was found to have a very strong temperature dependence, as shown in Fig. 7. The change in the temperature dependence of T_1 near T_{C1} (=387 K) is related to the loss of H_2O; the forms of the octahedra of water molecules surrounding Fe^{2+} are probably disrupted by the loss of H_2O.

Conclusions

The thermodynamic properties of $(NH_4)_2Fe(SO_4)_2{\cdot}6H_2O$ were investigated, and phase transitions were found at 387 and 500 K. This crystal loses H_2O with increasing temperature. The first mass loss occurs near 330 K (T_d), which is interpreted as the onset of partial thermal decomposition. The transformation anomalies at 387 K (=T_{C1}) and 500 K (=T_{C2}) are related to phase transitions from $(NH_4)_2Fe(SO_4)_2{\cdot}6H_2O$ to $(NH_4)_2Fe(SO_4)_2{\cdot}2H_2O$, and from $(NH_4)_2Fe(SO_4)_2{\cdot}6H_2O$ to $(NH_4)_2Fe(SO_4)_2{\cdot}H_2O$, respectively. From the ^1H $T_{1\rho}$ determined by MAS NMR and ^1H T_1 obtained in a single-crystal NMR experiment, the changes in the temperature dependence of $T_{1\rho}$ and T_1 near T_{C1} are associated with the structural phase transitions, which are due to the loss of H_2O and indicate that the forms of the octahedra of water molecules surrounding Fe^{2+} might be disrupted. This transformation is due to proton hopping and the breaking of hydrogen bonds. Near T_d, the relaxation time for the ^1H nuclei slowly decreases. This temperature is related to the beginning of the loss of H_2O, as observed in the TG results.

The abrupt change in $T_{1\rho}$ and T_1 near T_{C1} is the only detectable result of the structural transformation. T_1 and $T_{1\rho}$ are very short, on the order of milliseconds. The $T_{1\rho}$ and T_1 values of crystals containing paramagnetic ions are shorter than those of pure crystals; the influence of the paramagnetic ions is predominant. The relaxation time is expected to be inversely proportional to the square of the magnetic moment of the paramagnetic ion. Therefore, the $T_{1\rho}$ and T_1 values of materials containing Fe^{2+} ions are shorter than those of materials without paramagnetic ions. These short relaxation times indicate rapid energy transfer from the nuclear spin system to the surrounding environment.

Acknowledgements This research was supported by the Basic Science Research program through the National Research Foundation of Korea (NRF) funded by the Ministry of Education, Science, and Technology (2012001763).

References

1. Gronvold F, Meisingset KK. Thermodynamic properties and phase transitions of salt hydrates between 270 and 400 K I. $NH_4Al(SO_4)_2{\cdot}12H_2O$, $KAl(SO_4)_2{\cdot}12H_2O$, $Al_2(SO_4)_3{\cdot}17H_2O$, $ZnSO_4{\cdot}7H_2O$, $Na_2SO_4{\cdot}10H_2O$, and $Na_2S_2O_3{\cdot}5H_2O$. J Chem Therm. 1982;14:1083–98.
2. Lim AR, Lee JH. ^{23}Na and ^{87}Rb relaxation study of the structural phase transitions in the Tutton salts $Na_2Zn(SO_4)_2{\cdot}6H_2O$ and $Rb_2Zn(SO_4)_2{\cdot}6H_2O$ single crystals. Phys Status Solidi B. 2010;247:1242–6.
3. Jain VK, Venkateswarlu P. On the ^{57}Fe Mossbauer spectra of FeTe and Fe_2Te_3. J Phys C. 1979;12:865–73.
4. Marinova D, Georgiev M, Stoilova D. Vibrational behavior of matrix-isolated ions in Tutton compounds. II. Infrared spectroscopic study of NH_4^+ and SO_4^{2-} ions included in copper sulfates and selenates. J Mol Struct. 2009;938:179–84.
5. Marinova D, Georgiev M, Stoilova D. Vibrational behavior of matrix- isolated ions in Tutton compounds. I. Infrared spectroscopic study of NH_4^+ and SO_4^{2-} ions included in magnesium sulfates and selenates. J Mol Struct. 2009;929:67–72.
6. Marinova D, Georgiev M, Stoilova D. Vibrational behavior of matrix-isolated ions in Tutton compounds. IV. Infrared spectroscopic study of NH_4^+ and SO_4^{2-} ions included in nickel sulfates and selenates. Cryst Res Technol. 2010;45:637–42.
7. Georgiev M, Marinova D, Stoilova D. Vibrational behavior of matrix-isolated ions in Tutton compounds. III. Infrared spectroscopic study of NH_4^+ and SO_4^{2-} ions included in cobalt sulfates and selenates. Vib Spectrosc. 2010;53:233–8.
8. Riley MJ, Hitchman MA, Mohammed AW. Interpretation of the temperature dependent g values of the $Cu(H_2O)_6^{2+}$ ion in several host lattices using a dynamic vibronic coupling model. J Chem Phys. 1987;87:3766–78.
9. Hoffmann SK, Goslar J, Hilczer W, Augustyniak MA, Marciniak M. Vibronic behavior and electron spin relaxation of Jahn–Teller complex $Cu(H_2O)_6^{2+}$ in $(NH_4)_2Mg(SO_4)_2{\cdot}6H_2O$ single crystal. J Phys Chem A. 1998;102:1697–707.
10. Parthiban S, Anandalakshmi H, Senthilkumar S, Karthikeyan V, Mojumdar SC. Influence of Vo(II) doping on the thermal and optical properties of magnesium rubidium sulfate hexahydrate crystals. J Therm Anal Calorim. 2012;108:881–5.
11. Montgomery H, Lingafelter EC. The crystal structure of Tutton's salts. III. Copper ammonium sulfate hexahydrate. Acta Crystallogr. 1966;20:659–62.
12. Heilmann I, Knudsen JM, Olsen NB, Buras B, Olsen JS. Studies of thermal decomposition of $(NH_4)_2Fe(SO_4)_2{\cdot}6H_2O$. Solid State Commun. 1974;15:1481–4.
13. Ganesh G, Ramadoss A, Kannan PS, SubbiahPandi A. Crystal growth, structural, thermal, and dielectric characterization of Tutton salt $(NH_4)_2Fe(SO_4)_2{\cdot}6H_2O$ crystals. J Therm Anal Calorim. 2013;112:547–54.
14. Brown GM, Chidambaram R. The structure of copper ammonium sulfate hexahydrate from neutron diffraction data. Acta Crystallogr B. 1969;25:676–87.
15. Voight W, Goring S. Melting of Tutton's salts studied by DSC. Thermochim Acta. 1994;237:13–26.
16. Lim AR, Jeong SY. Phase transition in triglycine sulfate crystals by ^1H and ^{13}C nuclear magnetic resonance in the rotating frame. J Mole Struct. 2013;1048:471–5.
17. Lim AR, Shin HK. ^1H and ^7Li nuclear magnetic resonance study of the superionic crystals $K_4LiH_3(SO_4)_4$ and $(NH_4)_4LiH_3(SO_4)_4$. J Appl Phys. 2010;107:63513–8.